

Error Analysis of Bathymetric Data derived from IKONOS Imagery

Location: Tinian Island, Commonwealth of the Northern Marianas Islands

Produced by: Kyle R. Hogrefe: Hogrefe Natural Systems Analysis in affiliation with Davey Jones Locker GIS Laboratory, Oregon State University

Produced for: Pacific Islands Benthic Habitat Mapping Center (PIBHMC) / NOAA Fisheries' Coral Reef Ecosystem Division (CRED)

Analysis Overview

The derived bathymetry product that is the focus of this analysis differs from others delivered under this contract in that LiDAR data are used as the baseline dataset to establish spectral decay rate and as ground truth data to test the derived depths. Previous products used multibeam sonar data for these purposes. The presumed advantage of using the LiDAR dataset is that it provides coverage in shallow water (0 – 10m) while the scarcity data in this range has been considered a limitation of the multibeam data. Though Parts 1 and 2 demonstrate the improved accuracy of bathymetry derived using LiDAR as baseline data (when compared to the error analysis of the 12/19/08 product), Part 3 supports the accuracy of bathymetry derived using multibeam data as the baseline. This is significant because the desire to derive bathymetry from spectral data arises where LiDAR data are unavailable and its acquisition is cost prohibitive.

Bathymetric data were derived from IKONOS multispectral satellite imagery provided by the National Center for Coastal Monitoring and Assessment (NCCMA). The original imagery, purchased from Space Imaging, Inc. (now Geoeye, Inc.), was orthorectified to correct for detected geographic offsets. Three images, acquired on different dates, were analyzed to extend the spatial coverage of the final derived bathymetry product by combining data from cloud free areas. The image file names were “tinian_233_msi.pix”, “tinian_109297_msi_000_rat.img” and “tinian_109297_msi_001_rat”, but they will be referred to as Tin233, Tin297-00 and Tin297-01, respectively, in this analysis.

Processing steps were based on methods originating in Lyzenga 1985 with refinement as described in Hogrefe et al. 2008 and Hogrefe 2008

(<http://oregonstate.edu/~hogrefek/Cookbook/>).

An overview of the processing steps as follows:

- 1) Conversion of file type to view images
- 2) Data conversion from digital number to radiance values
- 3) Correction for atmosphere and water surface reflection
- 4) Linearization of spectral decay of as function of depth
- 5) Masking of data not applicable to depth derivation
- 6) Georectification of Images
- 7) Extraction of linearized spectral values and depth data
- 8) Perform multiple linear regression to determine formula variables for depth derivation (and derivation of depth)
- 9) Integration of derived bathymetry with multibeam sonar bathymetry

This analysis focuses on the statistical accuracy several products that result from step 8 to determine the most accurate data for integration with multibeam sonar bathymetry collected by PIBHMC/CRED and LiDAR data provided by the U.S. Navy. Once the multiple linear regression was performed in step 8 (above), the resulting variables were plugged into the multivariate slope intercept formula (below) to derive bathymetry. These variables can be adjusted to increase the accuracy and coverage of the product. The two basic changes in derived bathymetry that can be accomplished by adjusting the original multiple linear regression (MLR) variables are:

- 1) Depths can be changed equally across the entire image by adjusting the Y intercept. Depths are increased when the Y intercept is decreased and depths are decreased when the Y intercept is increased.
- 2) The slope of the regression line (of the derived depths against LiDAR depths) in the error analysis can be changed by adjusting the slope of the linearized blue and green spectral values. Thus, changing depths to varying degrees throughout the depth range.

These adjustments to the MLR variables allow for greater depth range and spatial coverage in the derived bathymetry. Depths derived in areas of very shallow water often have positive values which are then lost when the product is “trimmed” to include only depth (i.e. negative) values. I have hypothesized that this effect is due to an inversion of the spectral relationship between the blue and green bands in these very shallow areas. Where depths are greater than ~3 meters, blue radiance values are always greater than green radiance values, however, where depths are less than ~3 meters the inverse is often true. Because the multibeam bathymetry is seldom shallower than 10 m in the Tinian data, this “shallow inversion” was not captured in the values extracted for the multiple linear regression that determines the variables for depth derivation using multibeam data as the baseline. The LiDAR data available in the 0-10 m range seems to have captured the spectral decay relationship better leading to more accurate derived bathymetry. However the problem of positive values persisted to a lesser degree so that adjustments to the MLR variables were still required.

These adjustments also impact the statistical accuracy of the product. This error analysis validates the choice of which product(s) to integrate by establishing the statistical accuracy of derived bathymetry from each image using the original variables and then documents the statistical differences as the variables are adjusted.

The formula used to derive bathymetry is a multivariate slope intercept formula as follows:

$$\text{Depth} = Y_{\text{int}} + (m_{\text{blue}})(x_{\text{blue}}) + (m_{\text{green}})(x_{\text{green}})$$

Where:

Y_{int} = Y intercept

m = slope

x = linearized spectral value

Part 1: Analysis of Derived Bathymetry using Extraction Points.

In processing step 7, ArcGIS point features are created to extract LiDAR depth and linearized spectral values for use in the step 8 MLR analysis. Over 500 points are chosen per satellite image where pixels with clear spectral signal are concurrent with depths between 0 and 25 m. These same point features are used to extract derived depth values for comparison with LiDAR depth values in the following liner regression analyses. For image Tin233, 542 points were used while 501 points were used for image Tin297-00 and 666 points were used for image Tin297-01.

Image Tin233

As shown in Figure 1, the R^2 value for the bathymetry derived using the original MLR values is 0.7573 while the slope of the regression line is also 0.7573. This high R^2 value (approaching 1) represents a tight grouping of the derived depth scatter plot around its regression line while the high slope value indicates an excellent correlation between derived and LiDAR depth, represented by the (red) plot. The resulting raster grid provides very realistic bathymetric data, but its shortcoming is the aforementioned phenomenon of positive values in shallow areas.

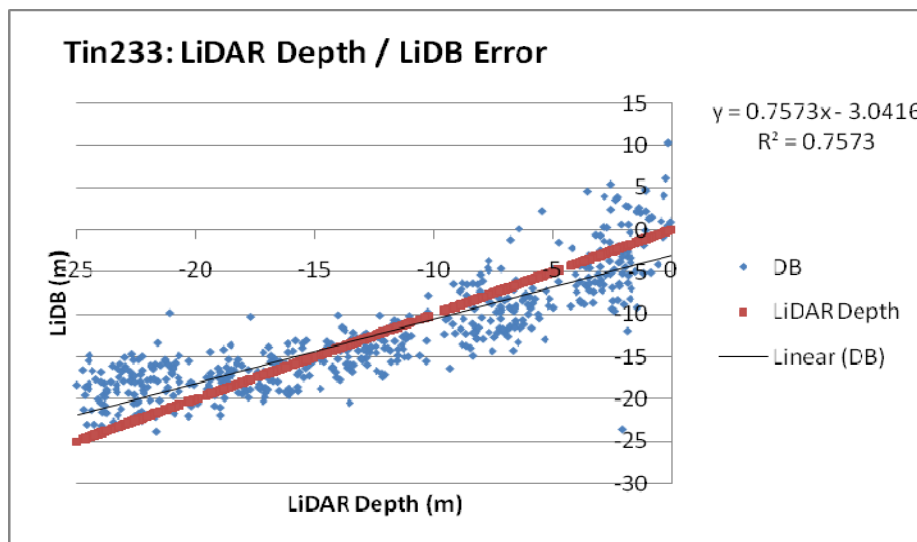


Figure 1. Error analysis of derived bathymetry from Tin233 using original MLR variables. Formula applied: $\text{Depth} = 15.9113 - 11.1089 * X_{\text{blue}} + 29.2445 * X_{\text{green}}$

In order to increase shallow coverage (0-5 m), new bathymetry was derived by both decreasing the Y-intercept (Figure 2) and then by simultaneously decreasing the slope values derived for the linearized blue and green spectral data (Figure 3). The decrease in Y-intercept increased depths “across the board” while resulting in more accurate derived values at greater depths. However, mid-range and shallow depths are made less accurate. The decrease of the slope of the linearized radiance values of both the blue and green bands, causes an increase in shallow depths with minimal changes to derived depth values from 15 to 25 meters. Both of these adjustments to the MLR variables result in an approximately 6 m increase in shallow depths (Note the similar Y-intercept values in Figures 2 and 3) and comparable increases to the spatial coverage of the derived product (detected by visual assessment).

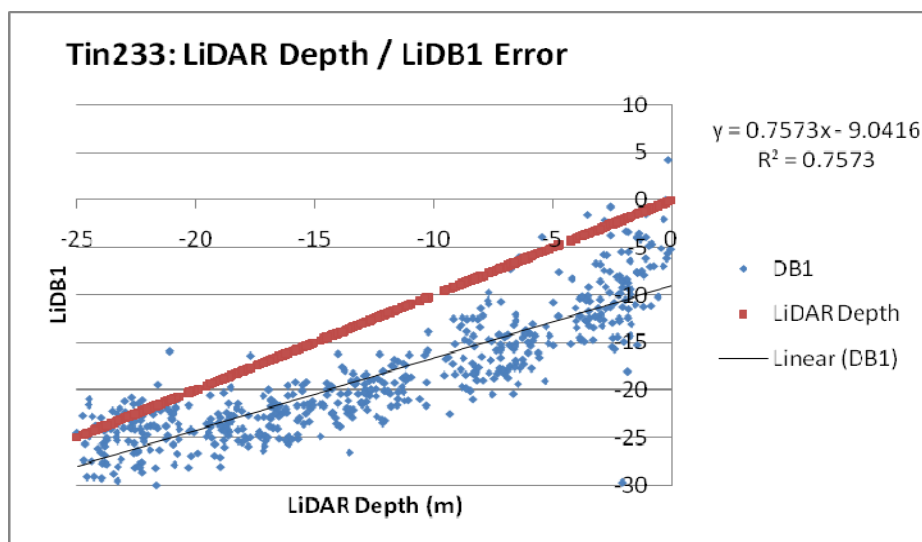


Figure 2. Error analysis of derived bathymetry from Tin233 using a decreased Y-intercept value. Formula applied: $\text{Depth} = 9.9113 - 11.1089 * X_{\text{blue}} + 29.2445 * X_{\text{green}}$

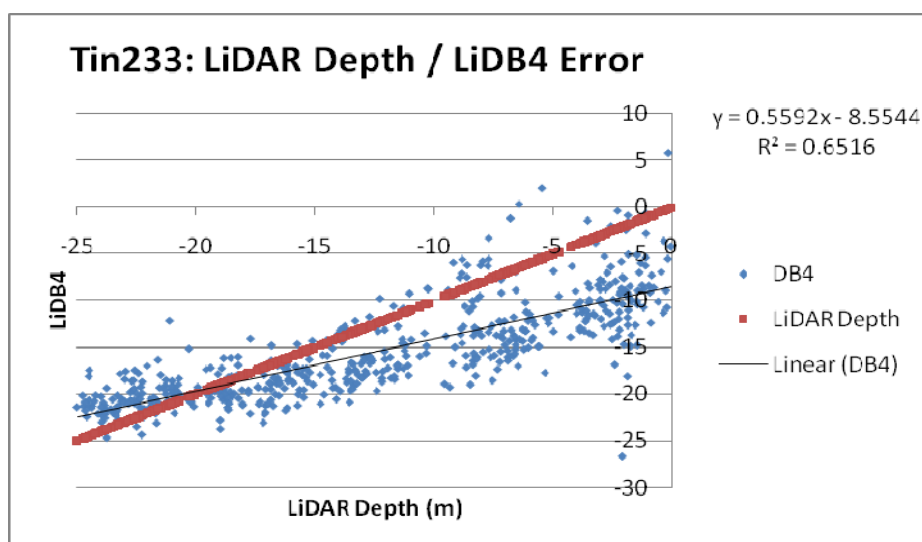


Figure 3. Error analysis of derived bathymetry from Tin233 using decreased blue and green slope values. Formula applied: $\text{Depth} = 15.9113 - 5.1089 * X_{\text{blue}} + 23.2445 * X_{\text{green}}$

In order to take advantage of the increased coverage in the 0-5 meter range achieved by adjusting the MLR variables while maintaining the accuracy in the original product, each of the two adjusted products were integrated with the original into a mosaic. During the mosaic, the data from the original product was prioritized over that from those with changed variables so that the more accurate data, in the 5-25 m range, was retained while the shallow water coverage was extended.

The statistical analyses of the Tin233-LiDB/DB1 and Tin233-LiDB/DB4 mosaiced products are provided in Part 2 (Figures 13 and 14).

Image Tin297-00

As shown in Figure 4, the R^2 value for the bathymetry derived using the original MLR values is 0.6568 while the slope of the regression line is also 0.6568. This R^2 value represents a tight grouping of the derived depth scatter plot around its regression line while the slope value indicates a high correlation between derived and LiDAR depth, represented by the (red) plot. The resulting raster grid provides realistic bathymetric data, but its shortcoming is the aforementioned phenomenon of positive values in very shallow areas.

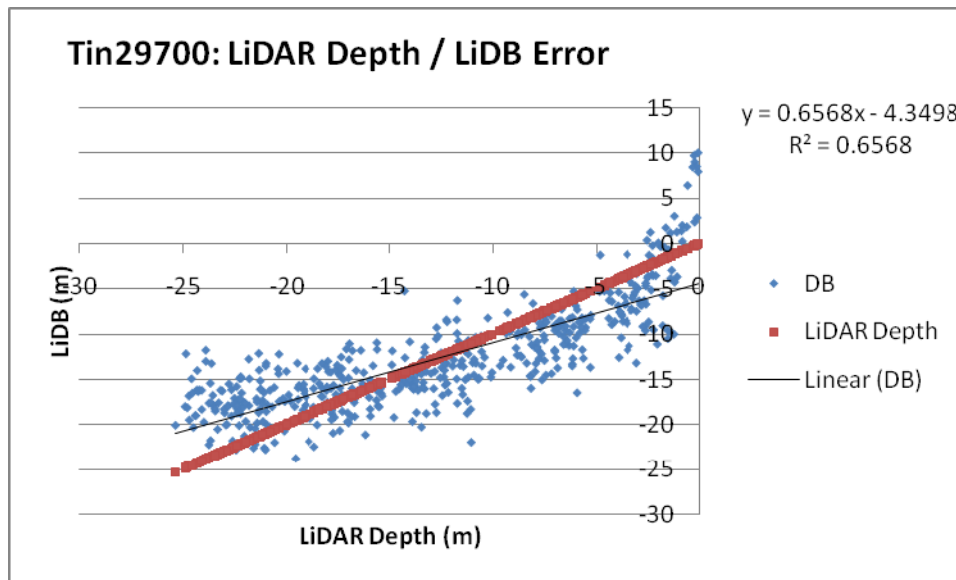


Figure 4. Error analysis of derived bathymetry from Tin297-00 using original MLR variables. Formula applied: $\text{Depth} = 6.8424 - 15.0336 * X_{\text{blue}} + 25.0675 * X_{\text{green}}$

In order to increase shallow coverage (0-5 m), new bathymetry was derived by both decreasing the Y-intercept (Figure 5) and then by simultaneously decreasing the slope values derived for the linearized blue and green spectral data (Figure 6). Though specific values vary, the effects of the changed variables exhibit the same patterns as described in the discussion of the Tin233 products (above).

Again, each of the two adjusted products was integrated with the original into a mosaic with the data from the original product prioritized over that from those with changed variables to increase coverage in shallow terrain without completely sacrificing the better statistical accuracy of the original.

The statistical analyses of the Tin29700-LiDB/DB1 and Tin29700-LiDB/DB4 mosaiced products are provided in Part 2 (Figures 18 and 19).

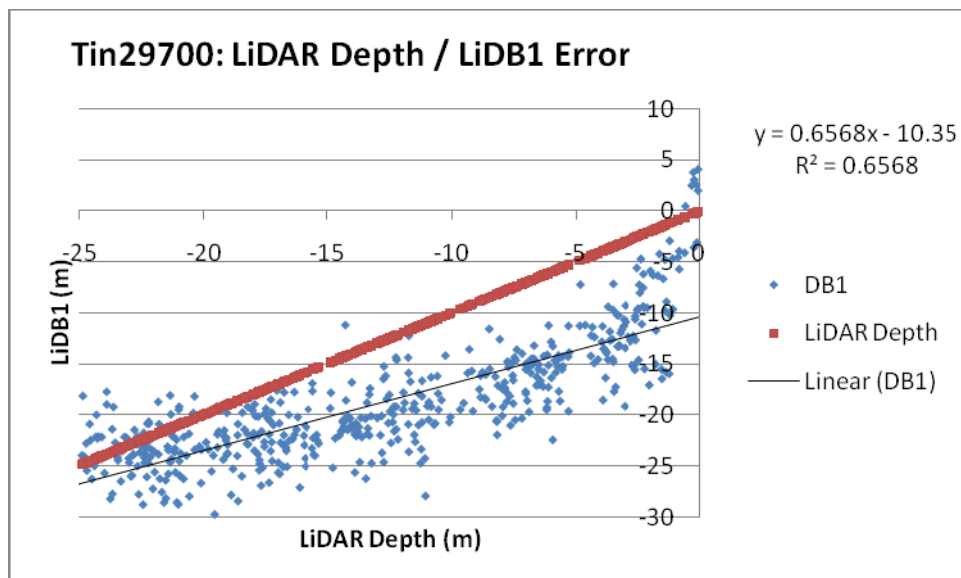


Figure 5. Error analysis of derived bathymetry from Tin297-00 using decreased Y-intercept value. Formula applied: $\text{Depth} = 0.8424 - 15.0336 * X_{\text{blue}} + 25.0675 * X_{\text{green}}$

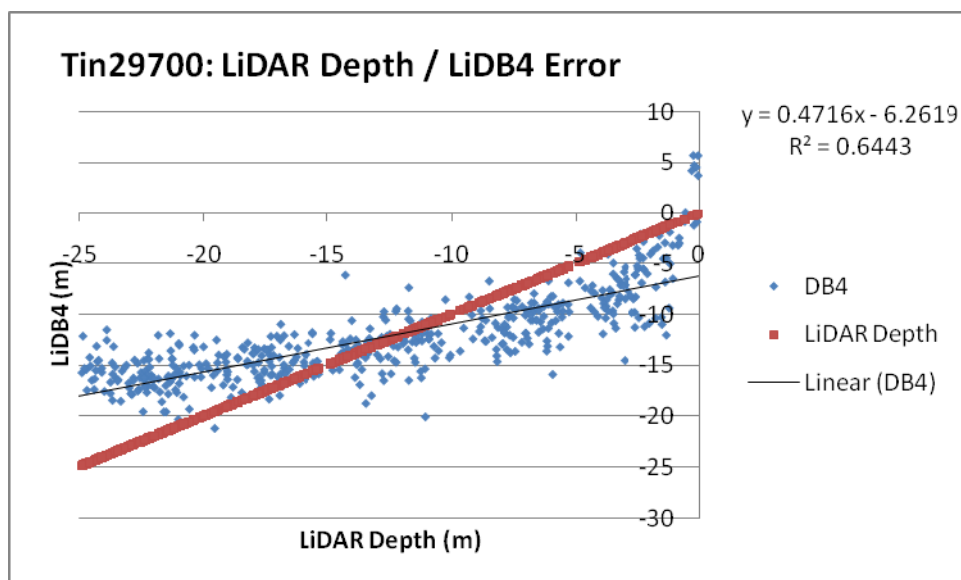


Figure 6. Error analysis of derived bathymetry from Tin297-00 using decreased blue and green slope values. Formula applied: $\text{Depth} = 6.8424 - 8.0336 * X_{\text{blue}} + 18.0675 * X_{\text{green}}$

Image Tin297-01

As shown in Figure 7, the R^2 value for the bathymetry derived using the original MLR values is 0.7575 while the slope of the regression line is also 0.7575. This high R^2 value represents a tight grouping of the derived depth scatter plot around its regression line while the slope value indicates high correlation between derived and LiDAR depth, represented by the (red) plot. The resulting raster grid provides very realistic bathymetric data, but its shortcoming is the aforementioned phenomenon of positive values in shallow areas.

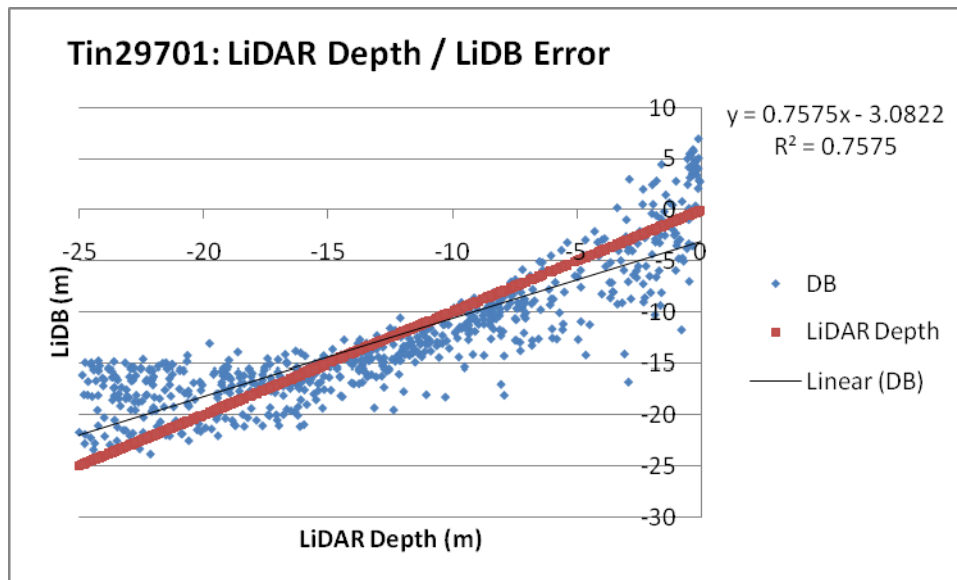


Figure 7. Error analysis of derived bathymetry from Tin297-01 using original MLR variables. Formula applied: $\text{Depth} = -1.5628 - 17.6634 * X_{\text{blue}} + 23.1723 * X_{\text{green}}$

In order to increase shallow coverage (0-5 m), new bathymetry was derived by both decreasing the Y-intercept (Figure 8) and then by simultaneously decreasing the slope values derived for the linearized blue and green spectral data (Figure 9). Though specific values vary, the effects of the changed variables exhibit the same patterns as described in the discussion of the Tin233 products (above).

Once again, each of the two adjusted products was integrated with the original into a mosaic with the data from the original product prioritized over that from those with changed variables to increase coverage in shallow terrain without completely sacrificing the better statistical accuracy of the original.

The statistical analyses of the Tin29701-LiDB/DB1 and Tin29701-LiDB/DB6 mosaiced products are provided in Part 2 (Figures 23 and 24).

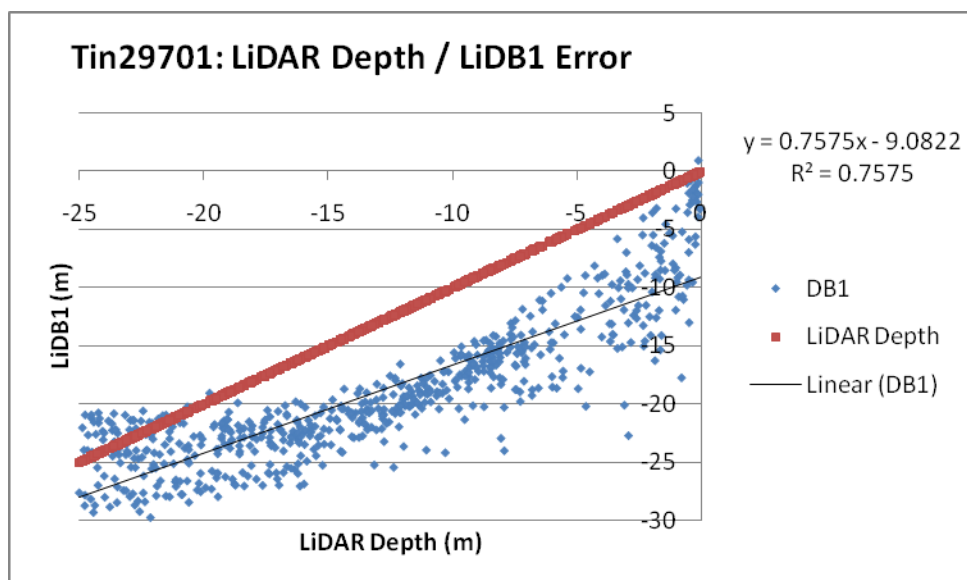


Figure 8. Error analysis of derived bathymetry from Tin297-01 using decreased Y-intercept values. Formula applied: $\text{Depth} = -7.5628 - 17.6634 * X_{\text{blue}} + 23.1723 * X_{\text{green}}$

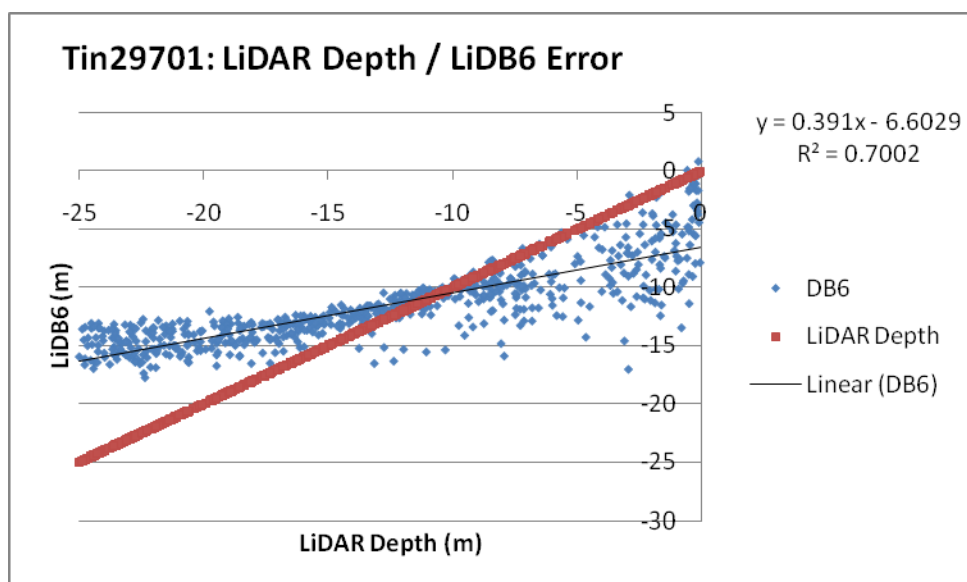


Figure 9. Error analysis of derived bathymetry from Tin297-01 using decreased blue and green slope values. Formula applied: $\text{Depth} = -1.5628 - 7.6634 * X_{\text{blue}} + 13.1723 * X_{\text{green}}$

Part 2: Analysis of Derived Bathymetry where Derived Depth Concurs with LiDAR Depths of less than 20 m.

The following analyses are a comprehensive statistical review of three derived bathymetry grids from each image as they are integrated to form a derived bathymetry mosaic, TinLiDBallMos. An analysis of this final derived bathymetry grid, which is subsequently integrated with the multibeam and LiDAR bathymetry into the product TinMBLiDBmos, is also included.

After the Part 1 analyses were conducted, the derived bathymetry raster grids were prepared for integration with by applying masks to exclude:

- 1) Derived depths of greater than 25 meters or less than 0 meters
- 2) Values derived from island areas and areas of cloud cover
- 3) Depths derived in areas deeper than 25 meters as indicated by the LiDAR bathymetry
- 4) Values derived inside the Tinian coastline as indicated by a shapefile provided by the NCCMA with the IKONOS imagery.

All remaining values were considered to be potentially valid derived depths; however, derived data deeper than 20 m are seldom used because the multibeam data usually reaches shallower depths. Therefore, the following error analyses utilize the derived and sonar depth values of each grid cell where derived data overlaps with multibeam sonar data of 20 m or less. Microsoft Excel was used for these analyses. However, because the Tinian multibeam data is deeper than 20 m for much of the island's perimeter, TinMBLiDBmos includes derived depths up to the derivation methodology's limit of 20-25 meters. The final graph in this section analyzes the error of the full 0-25 m depth range.

Extraction of all depth values where the trimmed derived bathy grid and LiDAR bathy grid overlap lead to datasets of up to 300,000 points. Subsets containing 10,000 points to compare derived and LiDAR data were determined to be sufficient and were created using a systematic (every Nth point) sample frame.

Helpful notes:

Figures 10, 11 and 12 analyze the same product as Figures 1, 2 and 3: bathymetry derived from image Tin233 using original MLR variables, reduced Y-intercept and reduced linearized blue and green band slope values, respectively.

Figures 15, 16 and 17 analyze the same product as Figures 4, 5 and 6: bathymetry derived from image Tin297-00 using original MLR variables, reduced Y-intercept and reduced linearized blue and green band slope values, respectively.

Figures 20, 21 and 22 analyze the same product as Figures 7, 8 and 9: bathymetry derived from image Tin297-01 using original MLR variables, reduced Y-intercept and reduced linearized blue and green band slope values, respectively.

Image Tin233

For the derived bathymetry products from the image Tin233 presented in Figures 10, 11 and 12, the R^2 and slope values for the derived products are reduced to a small degree (from Part 1) due to greater variability in departure from the mean value when all derived depth less than 20 m are considered. This is due to the variable sea state and cloud cover in this image adding to the inherent variability in the derived depth data when considering $\sim 10,000$ data points. However, this reduction is to a much lesser degree than for past products, presumably due to the consideration of data from shallow depths when establishing the spectral decay relationship and in the error analysis.

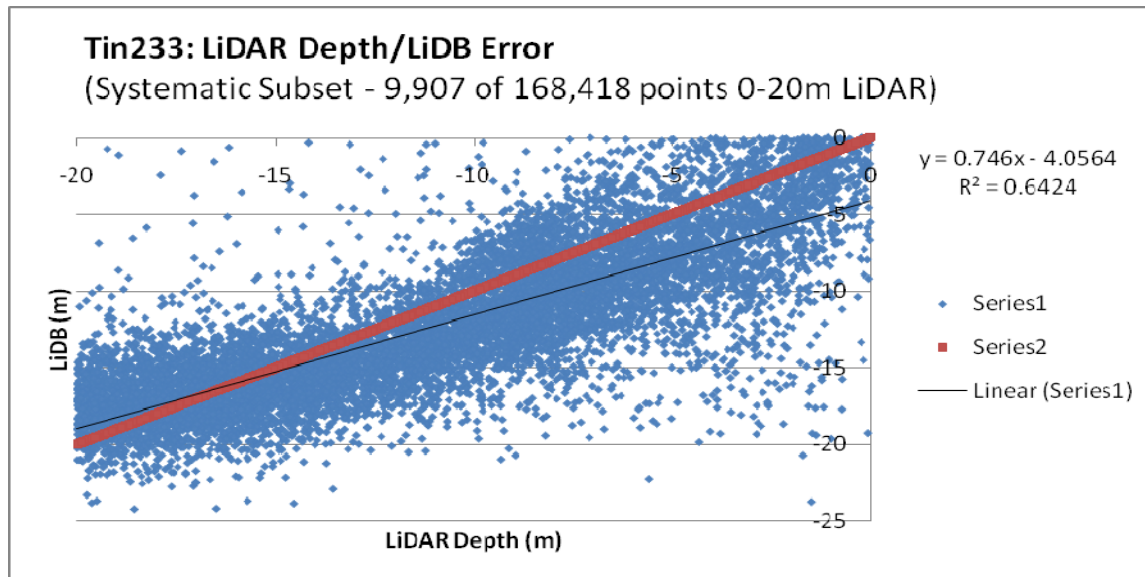


Figure 10. Comprehensive error analysis of derived bathymetry from Tin233 using original MLR variables. Formula applied: $\text{Depth} = 15.9113 - 11.1089 * X_{\text{blue}} + 29.2445 * X_{\text{green}}$

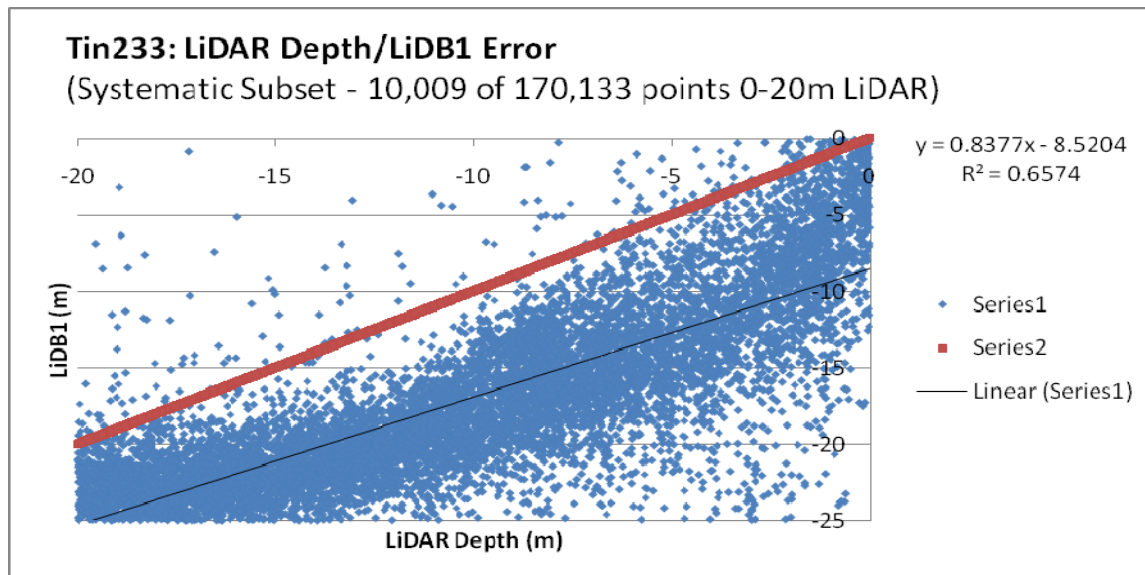


Figure 11. Comprehensive error analysis of derived bathymetry from Tin233 using decreased Y-intercept value. Formula applied: $\text{Depth} = 9.9113 - 11.1089 * X_{\text{blue}} + 29.2445 * X_{\text{green}}$

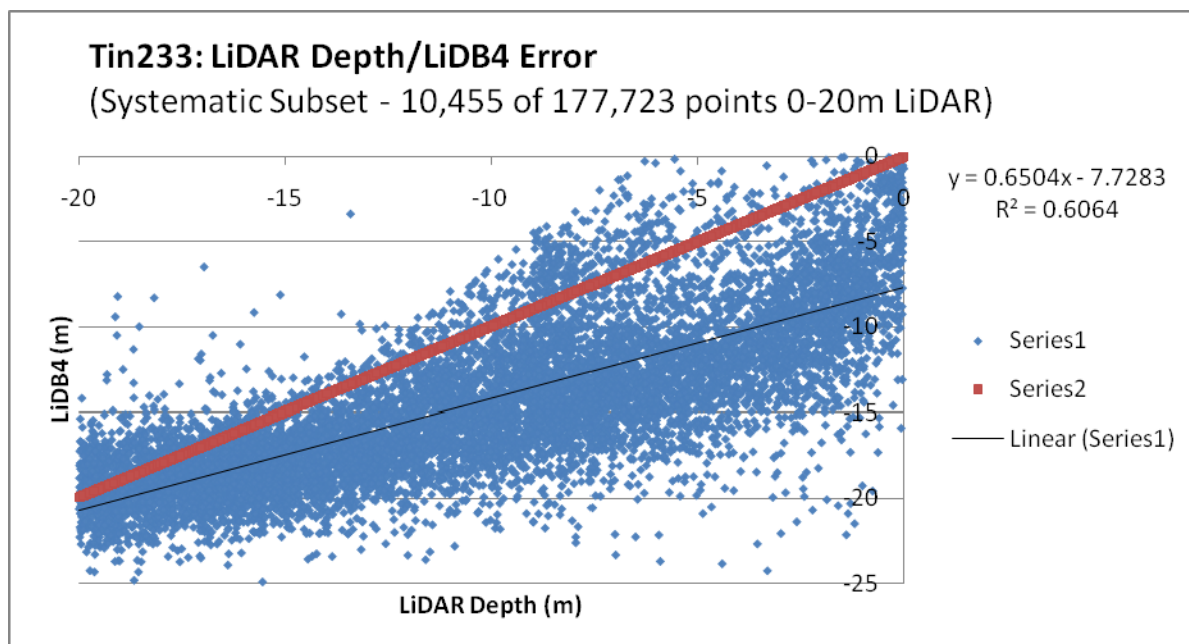


Figure 12. Comprehensive error analysis of derived bathymetry from Tin233 using decreased blue and green slope values. Formula applied: $\text{Depth} = 15.9113 - 5.1089 * X_{\text{blue}} + 23.2445 * X_{\text{green}}$

Both products that resulted from adjusted variables, DB1 and DB4, were mosaiced with the original product, DB, to expand spatial coverage in shallow areas.

Considering the derived bathymetry mosaic Tin233_LiDBDB1_mos (Figure 13), the statistical accuracy of the integrated product decreases slightly from that of the original product (Figure 10) with a decreased R^2 value while the statistical accuracy of the derived bathymetry mosaic Tin233_LiDBDB4_mos (Figure 14) actually increases over that of the original product with an increased R^2 . However this difference is slight and the lower Y-intercept values in figure 13 indicates that the LiDBDB1 derivations are more correlated to the LiDAR depths.

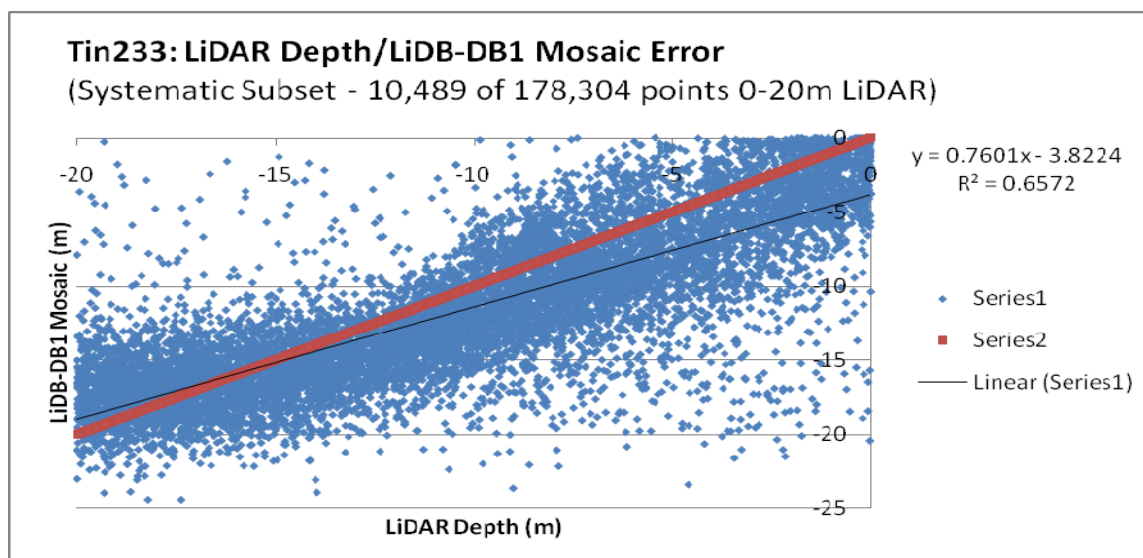


Figure 13. Comprehensive error analysis: mosaic of derived bathymetry products DB and DB1.

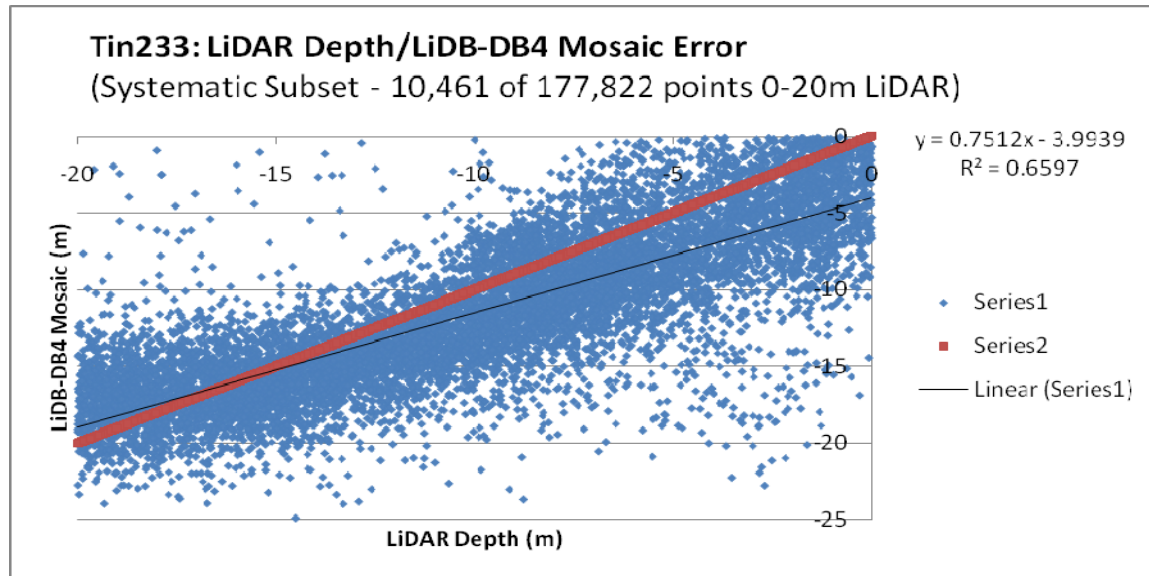


Figure 14. Comprehensive error analysis: mosaic of derived bathymetry products DB and DB4.

Given the results of these statistical analyses, the derived bathymetry mosaic Tin233_LiDBDB1_mos is considered to be the best product for eventual integration with LiDAR and multibeam bathymetry. However, large areas of shallow water terrain were obscured by cloud cover in this image. Images Tin297-00 and Tin297-01 also have significant cloud cover, but many of areas obscured in Tin233 were cloud free. Bathymetry was also derived from these images to extend spatial coverage of the final product.

Image Tin297-00

For the derived bathymetry products from the image Tin297-00 presented in Figures 15, 16 and 17, the R^2 values for the derived products are reduced a bit (from Part 1) due to a greater variability in departure from the mean value when all derived depth less than 20 m are considered. This is due to the moderate sea state and cloud cover in this image adding to the inherent variability in the derived depth data when considering more points. Both of the changes to MLR variables lead to comparable impacts to statistical accuracy as judges by R^2 value.

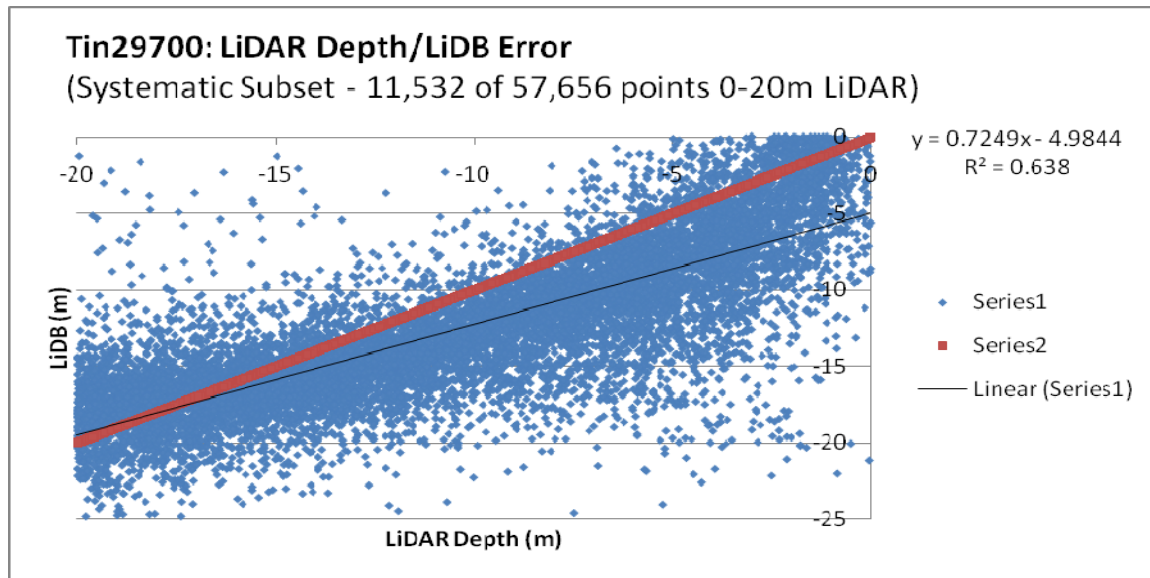


Figure 15. Comprehensive error analysis of derived bathymetry from Tin297-00 using original MLR variables. Formula applied: $\text{Depth} = 6.8424 - 15.0336 * X_{\text{blue}} + 25.0675 * X_{\text{green}}$

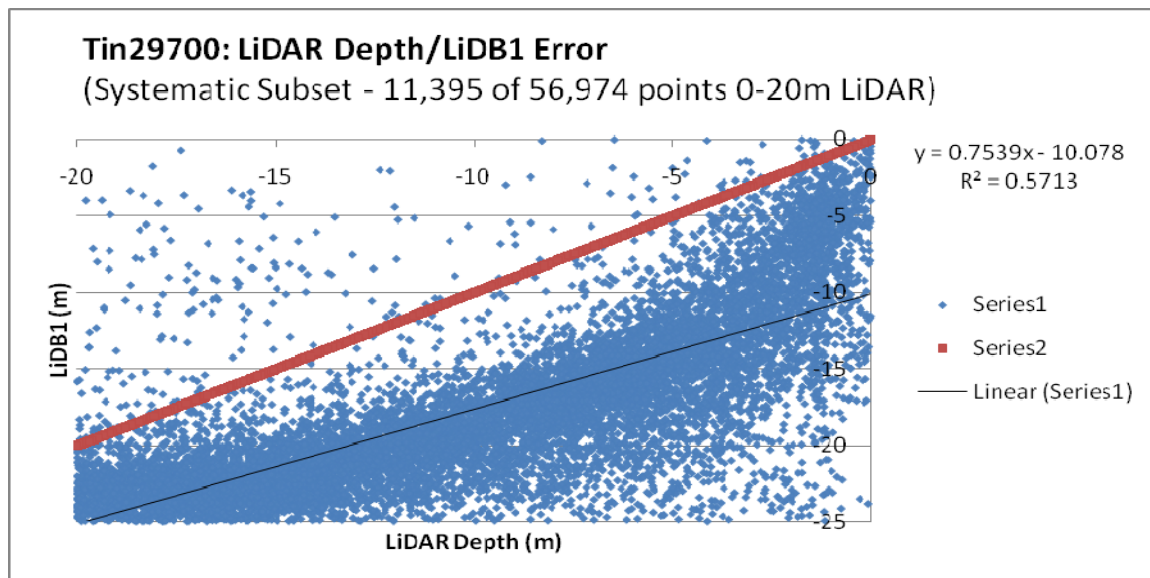


Figure 16. Comprehensive error analysis of derived bathymetry from Tin297-00 using decreased Y-intercept value. Formula applied: $\text{Depth} = 0.8424 - 15.0336 * X_{\text{blue}} + 25.0675 * X_{\text{green}}$

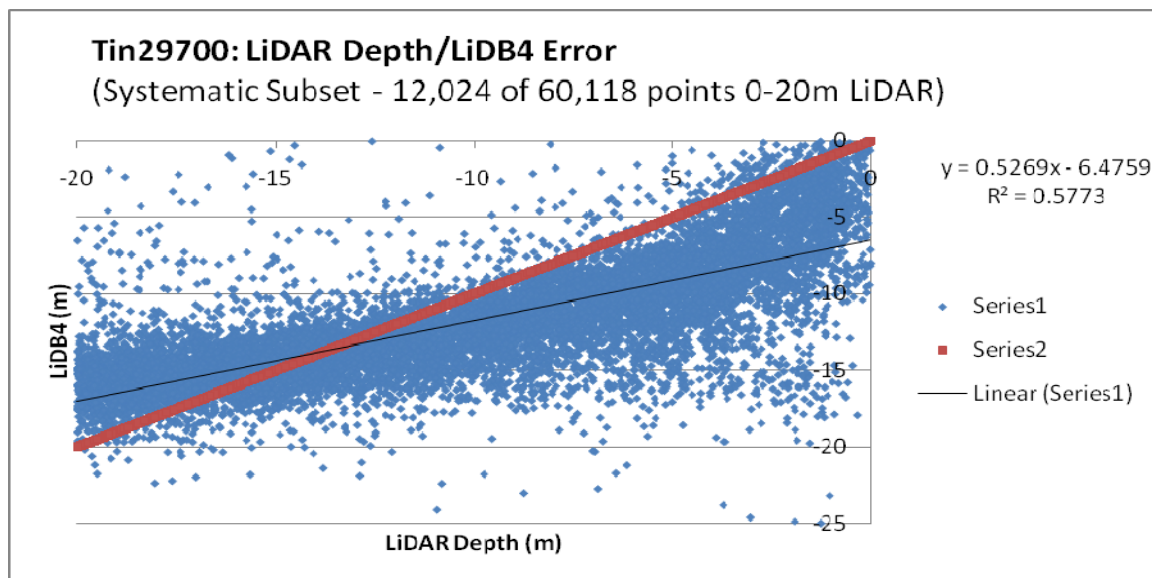


Figure 17. Error analysis of derived bathymetry from Tin297-00 using decreased blue and green slope values. Formula applied: $\text{Depth} = 6.8424 - 8.0336 * X_{\text{blue}} + 18.0675 * X_{\text{green}}$

Both products that resulted from adjusted variables, DB1 and DB4, were mosaiced with the original product, DB, to expand spatial coverage in shallow areas.

Considering the derived bathymetry mosaic Tin29700_LiDBDB1_mos (Figure 18), the statistical accuracy of the integrated product decreases from that of the original product (Figure 15) with significantly decreased R^2 and Y-intercept values. However, the statistical accuracy of the derived bathymetry mosaic Tin29700_LiDBDB4_mos (Figure 19) only decreases slightly in both measures.

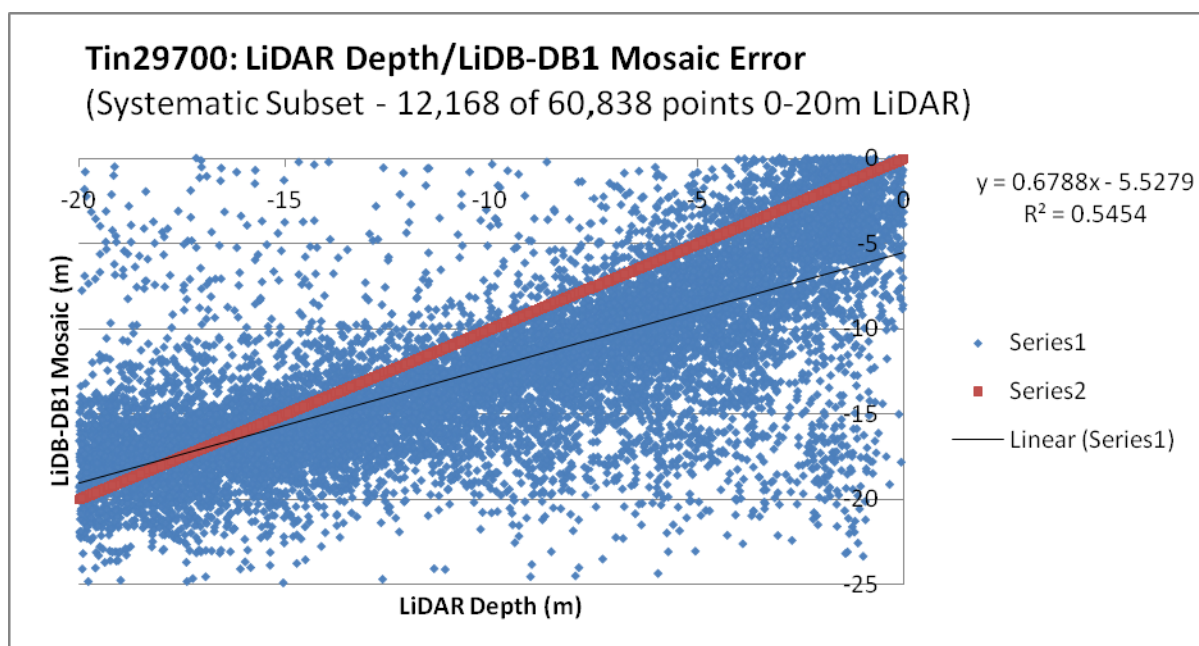


Figure 18. Comprehensive error analysis: mosaic of derived bathymetry products DB and DB1.

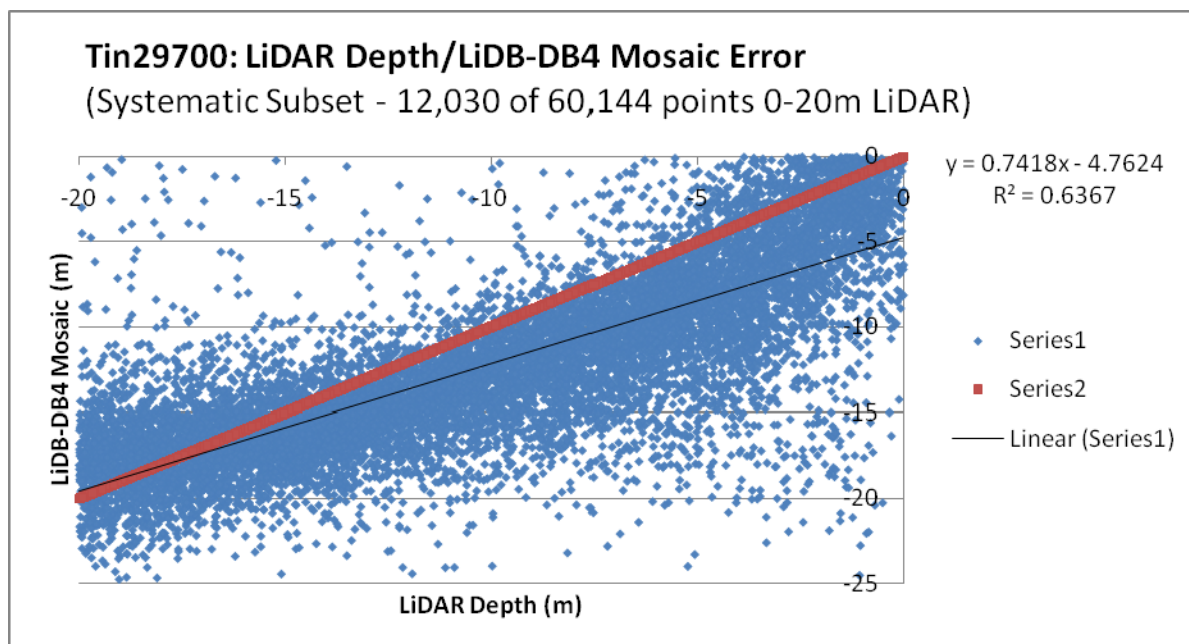


Figure 19. Comprehensive error analysis: mosaic of derived bathymetry products DB and DB4.

Given the results of these statistical analyses, the mosaic of derived bathymetry products DB and DB4 from image Tin297-00 is considered to be the best product for eventual integration with LiDAR and multibeam bathymetry.

Image Tin297-01

For the derived bathymetry products from the image Tin297-01 presented in Figures 20, 21 and 22, the R^2 values for the derived products are reduced somewhat (from Part 1) due to a greater variability in departure from the mean value when all derived depth less than 20 m are considered. This is due to the variable sea state and cloud cover in this image adding to the inherent variability in the derived depth data when considering over 10,000 data points. However, notice that the slope value increases in each case when more points are considered. This indicates that the slope of the scatterplot trend line more closely matches the 1:1 relationship of the sonar depth plotted against itself, a better reflection of reality.

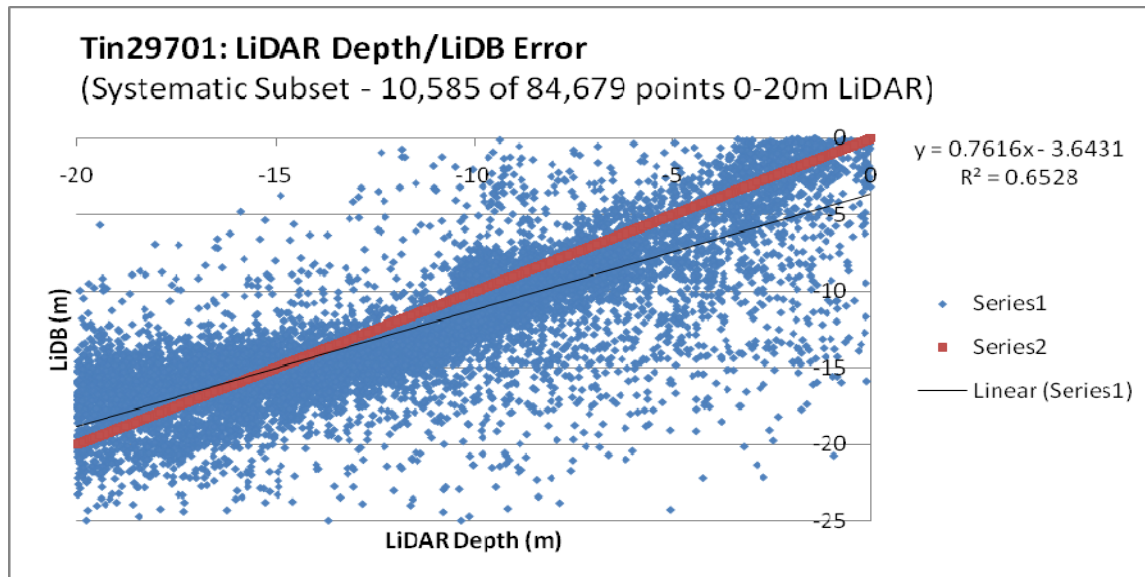


Figure 20. Comprehensive error analysis of derived bathymetry from Tin297-01 using original MLR variables. Formula applied: $\text{Depth} = -1.5628 - 17.6634 * X_{\text{blue}} + 23.1723 * X_{\text{green}}$

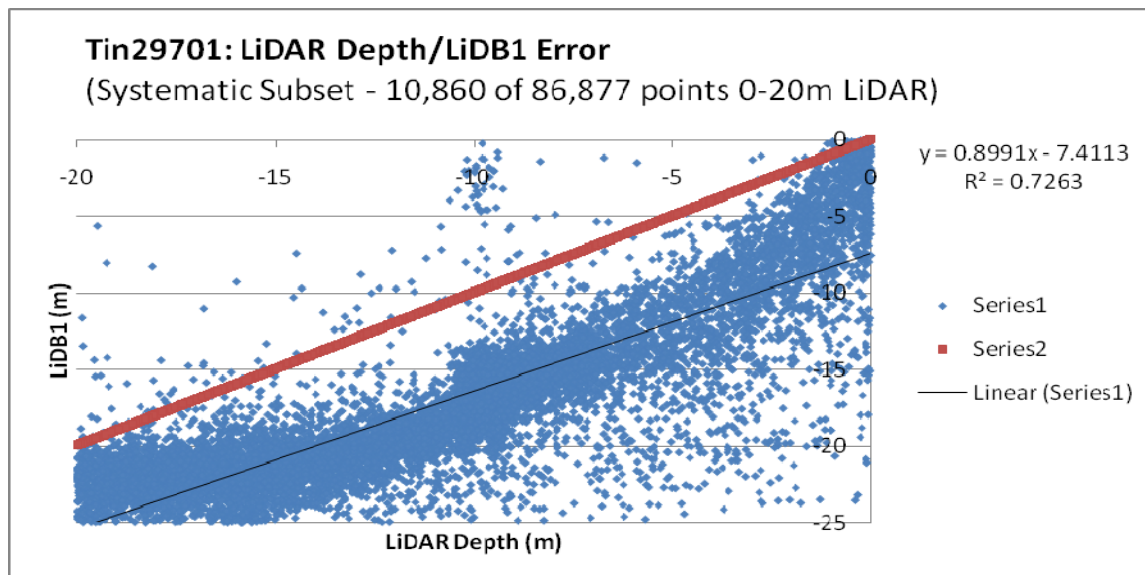


Figure 21. Comprehensive error analysis of derived bathymetry from Tin297-01 using decreased Y-intercept values. Formula applied: $\text{Depth} = -7.5628 - 17.6634 * X_{\text{blue}} + 23.1723 * X_{\text{green}}$

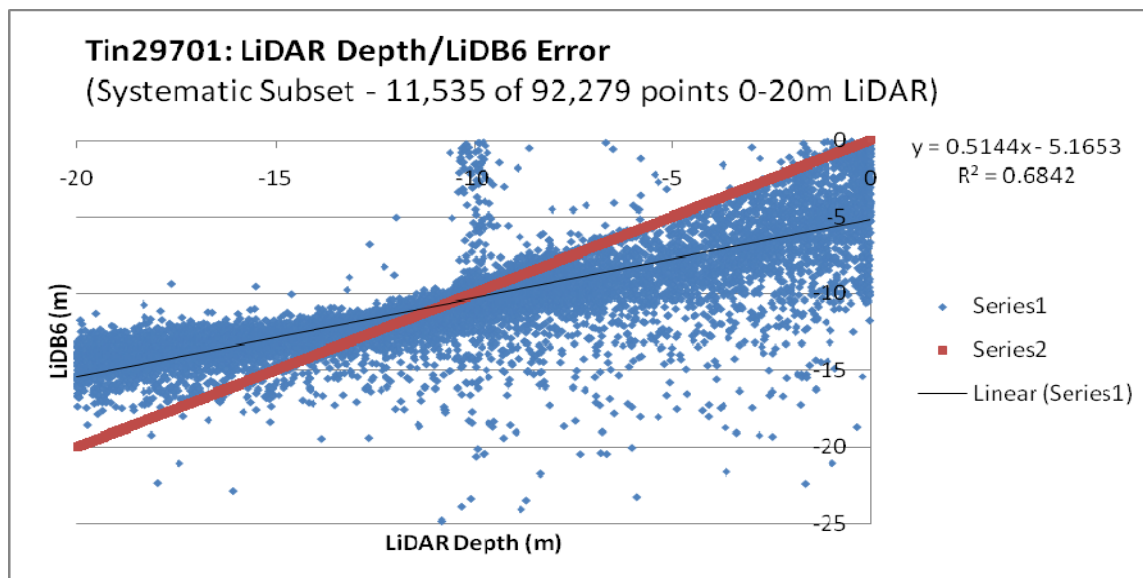


Figure 22. Comprehensive error analysis of derived bathymetry from Tin297-01 using decreased blue and green slope values. Formula applied: $\text{Depth} = -1.5628 - 7.6634 * X_{\text{blue}} + 13.1723 * X_{\text{green}}$

Both products that resulted from adjusted variables, DB1 and DB6, were mosaiced with the original product, DB, to expand spatial coverage in shallow areas.

Considering the derived bathymetry mosaic Tin29701_LiDBDB1_mos (Figure 23), the statistical accuracy of the integrated product actually increases significantly from that of the original product (Figure 20) with increased R^2 and Y-intercept values. The statistical accuracy of the derived bathymetry mosaic Tin29701_DBDB6_mos (Figure 24) also increases, but to a lesser degree.

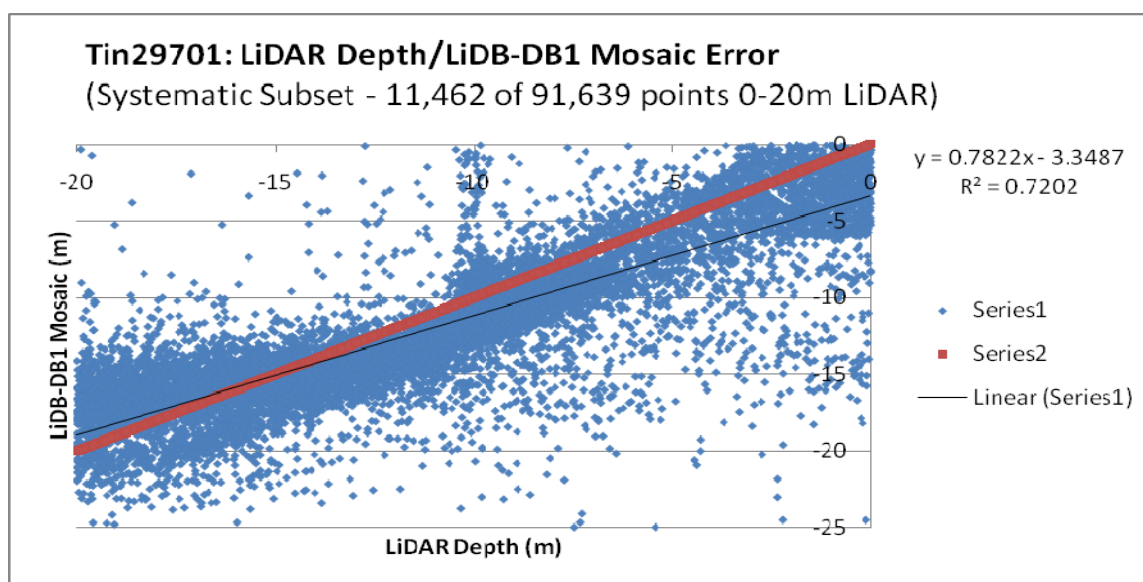


Figure 23. Comprehensive error analysis: mosaic of derived bathymetry products DB and DB1.

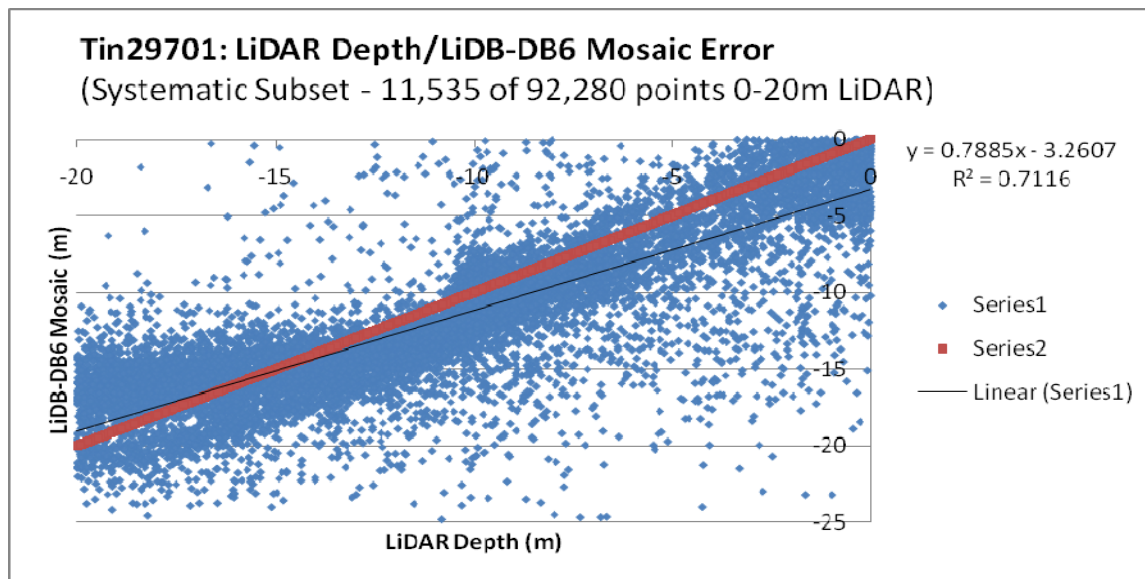


Figure 24. Comprehensive error analysis: mosaic of derived bathymetry products DB and DB6.

Given the results of these statistical analyses, the mosaic of derived bathymetry products DB and DB1 from image Tin29701 is considered to be the best product for eventual integration with LiDAR and multibeam bathymetry.

Final Mosaics of Derived Bathymetry from all Images

In order to achieve the greatest spatial coverage possible, the derived bathymetry mosaics from each image were in turn mosaiced for the final integration. During integration first priority was given to the product data from image Tin29701 (tin229701_LiDBDB1_mos) since it was the most statistically accurate. Second priority was given to the data product from Tin233 (tin233_LiDBDB1_mos) and third priority to the data product from Tin29700 (tin29700_DBDB4_mos). Data from higher priority datasets replaces that from lower priorities when data are concurrent during integration.

Statistical analyses (Figures 25 and 26) and visual inspection of this integrated product demonstrate a high degree of statistical validity and excellent representation of near shore terrain. Note that the statistics for this final product (TinLiDBallMos) indicate comparable or superior accuracy to the interim products that were derived from either original or adjusted MLR variables.

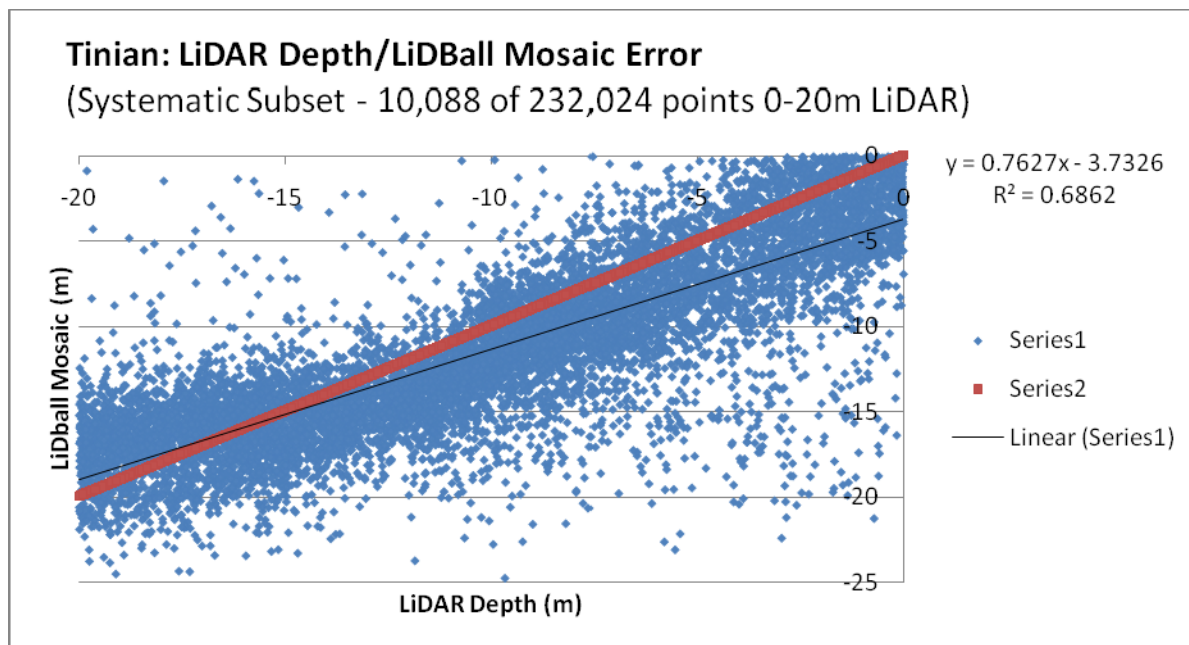


Figure 25. Comprehensive error analysis: integration of derived bathymetry mosaics from all three images to 20 m.

Because the Tinian multibeam data did not cover shallows very well for most of the island's perimeter, the final multibeam/LiDAR/derived bathymetry mosaic includes derived depths up to 25 m. Thus, the accuracy of derived depth up to 20 m and 25 m were assessed in Figure 26.

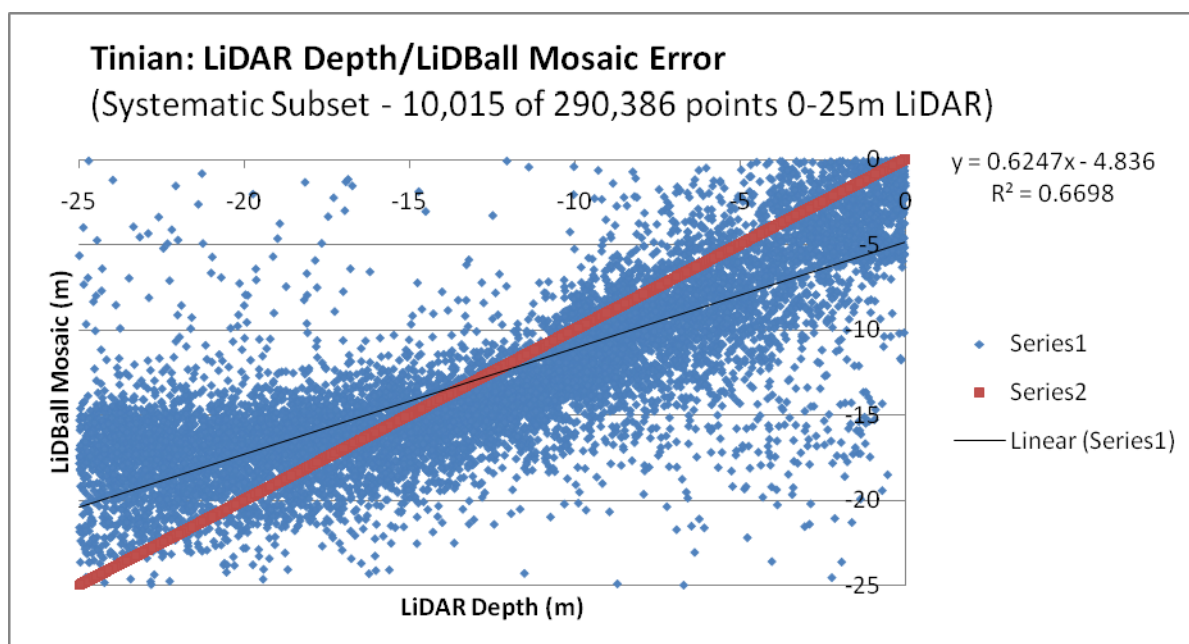


Figure 26. Comprehensive error analysis: integration of derived bathymetry mosaics from all three images to 25 m.

Part 3: Analysis of Bathymetry Derived with Multibeam Data as Baseline using LiDAR Data as ground truth

A comparison of this error analysis with the one submitted for the 12/19/08 deliverable makes it easy to assume that the product derived using LiDAR as a baseline is far superior to the product derived using multibeam sonar as a baseline. Comparing R^2 values of the final derived bathymetry mosaics, 0.6862 for LiDAR based derivations (above) and 0.2575 for multibeam based derivations (previous analysis) seems to make this clear. However, the dearth of multibeam datapoints in the shallows has not only presented a challenge in establishing spectral decay rate with depth, but also with error assessment. A strength of bathymetric derivations using spectral data is that it allows for depth data in areas that are hard to get to because of shallow depths as long as some control points exist nearby – i.e. deeper water. But how accurate are these shallow depths (0-5 m) when they are derived from a spectral decay relationship established with data from deeper depths (10-25 m)? This question is particularly germane to the Tinian data because multibeam sonar depths shallower than 10 m were scarce.

To answer this question, the LiDAR bathymetry dataset was used to analyze the error associated with the bathymetry derived based on multibeam data. As in Part 2, depth data were extracted for each raster cell where LiDAR data and the derived bathymetry mosaic delivered on 12/18/08 overlapped. As can be clearly surmised from Figures 27 and 28, though the bathymetry data derived based on LiDAR is more statistically accurate, the bathymetry data derived based on multibeam bathymetry is not only statistically valid, but comparable in its accuracy. This is despite the paucity of depths shallower than 10 m in the multibeam dataset. The difference in the statistical outcome of this error analysis (using LiDAR) and the 12/18/08 error analysis (using multibeam) is presumed to be that there were simply no shallow data points to be considered so that the statistical correlation could not be established.

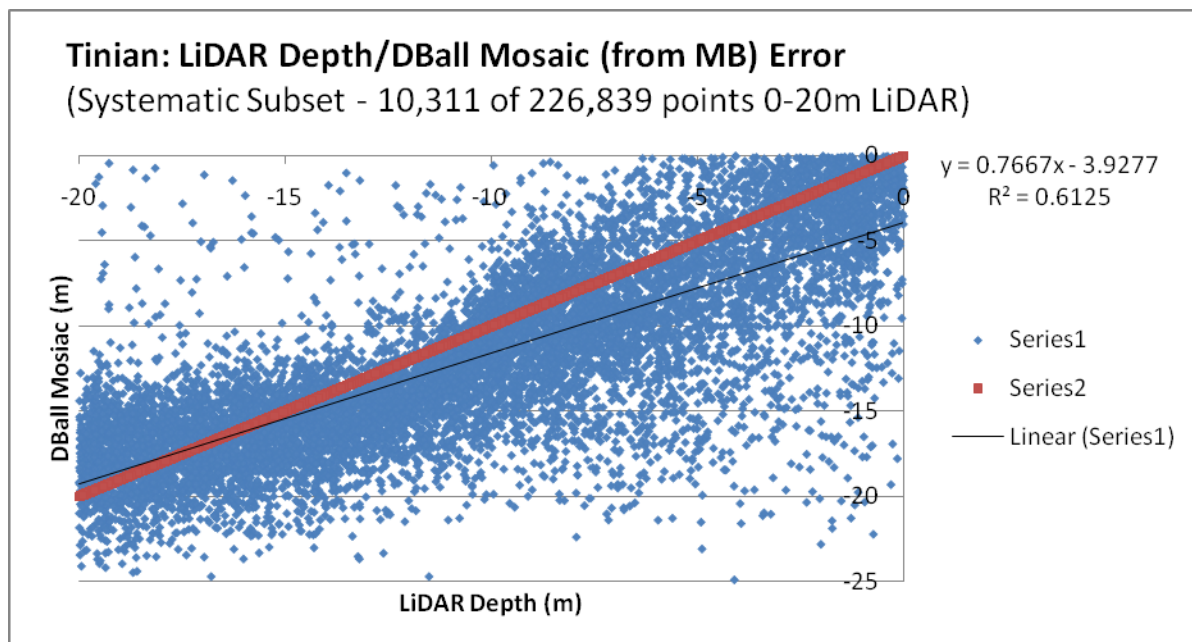


Figure 27. Comprehensive error analysis: mosaic of derived bathymetry based off of multibeam sonar data against LiDAR depth to 20 m.

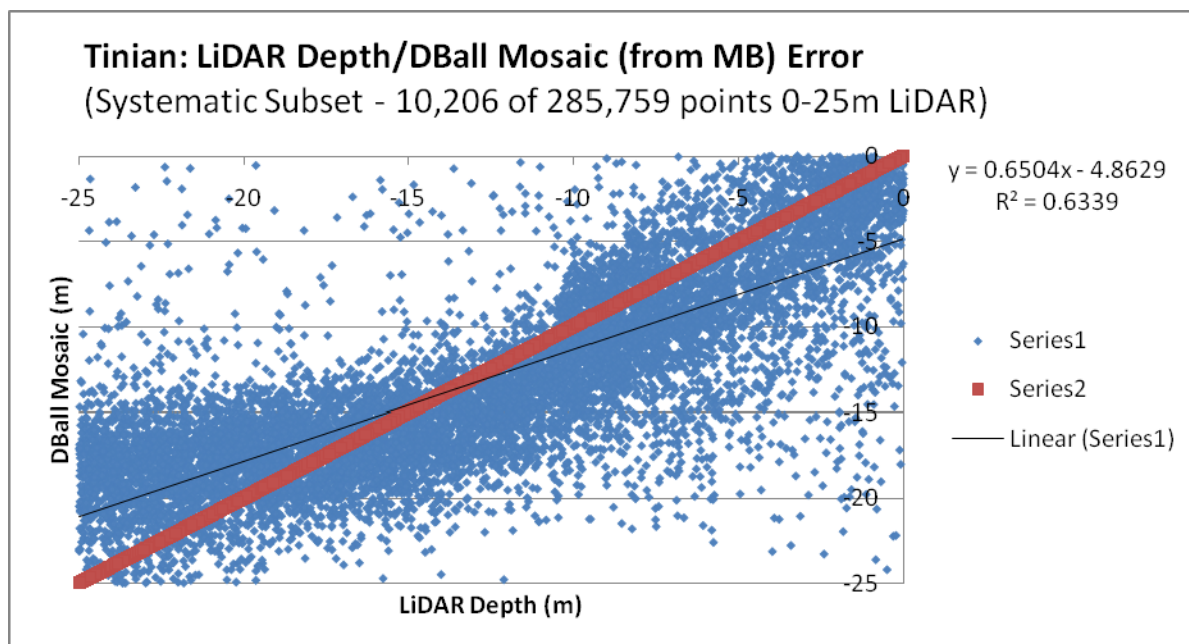


Figure 28. Comprehensive error analysis: mosaic of derived bathymetry based off of multibeam sonar data against LiDAR depth to 25 m.

This final analysis demonstrates the accuracy and efficacy of using multispectral satellite imagery to derive bathymetry, even if very shallow depths are not available when establishing the differential decay rate of the blue and green bands. Though the R^2 values of the depths derived using multibeam as a baseline are smaller than those using LiDAR as a baseline, they can be considered statistically comparable in their accuracy assessment.